Chapter 6

Extension of Molecular Dynamics, Enhanced Sampling and the Free-Energy Calculations

The atomistic level MD method as introduced in the previous chapter allows us to simulate the propagation of a system using a finite time step so that the total energy of this system is conserved and the temperature is under control. This means that the propagation needs to be done with a time interval in order of femtosecond, or even shorter. Processes of real chemical interest, however, happen on a much longer time-scale. Taking the *ab initio* MD simulation of some molecules being adsorbed on a metal surface as an example, currently, it takes a powerful computer cluster with a few hundreds of processors roughly one month to simulate the MD propagation of 100 ps [286]. Imagining that we want to see a rare-event chemical reaction happening with a time-scale of one millisecond, we need to continue this simulation on this cluster for about 10^6 years in order to see this event happening once. Even if the *ab initio* method is renounced in descriptions of the inter-atomic interactions, rather, the empirical potentials are used so that the MD simulation can propagate for, say 100 nano-second a day, reproducing the propagation of 1 millisecond still requires computer simulation of about 30 years. Plus, several times this event needs to happen in order for the statistics to work. Therefore, from a statistical point of view, the bruteforce MD technique is completely unacceptable in practical simulations involving such rare events. A better scheme, in which rare event like this can be simulated, is highly desired.

During the past years, great effort has been made in order for this purpose to be fulfilled. One route is to give up the all-atom description and use a coarse-grained model [287, 288]. In so doing, the time step used for the MD simulation can be significantly increased so that the time scale accessible to computer simulations increases, sometimes to a value large enough to complement biological or chemical

experiments. However, it is worth noting that an *a priori* detailed knowledge of the system to be simulated is required, which unfortunately is often not available.

A different route, which keeps the atomistic feature for the description of the propagation, is to develop a method so that the frequency with which rave event happens can be significantly increased. Or, in other words, an enhanced sampling efficiency is guaranteed. Over the last almost 4 decades, great success has been achieved in this direction. A number of methods, e.g. the umbrella sampling [94, 95], the adaptive umbrella sampling [33], the replica exchange [34, 35], the metadynamics [38, 39], the multi-canonical simulations [40, 41], the conformational flooding [42], the conformational space annealing [43], the integrated tempering sampling [44, 45, 46, 47] methods, etc. had been proposed, each having its own strength and weakness. For example, in the umbrella sampling, adaptive umbrella sampling, metadynamics, and configurational flooding methods, pre-determined reaction coordinates are required before the simulations were carried out. While in replica exchange and multi-canonical simulations, different temperature simulations are needed, which makes the trajectories obtained losing their dynamical information. In this chapter, we will take the umbrella sampling, the adaptive umbrella sampling, and the metadynamics methods as examples of the former class to show how they work in practice. In addition to this, the integrated tempering sampling method from the second class will also be discussed.

The enhanced sampling methods as introduced above focus on exploring the free-energy profile, or otherwise often called potential of mean force (PMF), throughout the entire conformational phase space of the poly-atomic system under investigation. In some applications of the molecular simulations, e.g. phase transitions, this entire PMF exploration can be avoided if the two competing phases are well-defined meta-stable states in standard MD simulations. In such cases, the free-energy of the system at each phase can be calculated using methods like thermodynamic integration, as a certain temperature and pressure. Then, by monitoring the competition of these two free-energies at different temperatures and pressures, one can find out which phase is more stable at a certain condition and consequently determine the phase diagram of this substance under investigation. Since phase transition is also an important topic in molecular simulations, principles underlying the thermodynamic integration method will also be explained in this chapter. We note that although this is the motivation for our explanation of the thermodynamic integration method, the range of its applications is much wider than this. As a matter of fact, the principles underlying this idea of thermodynamic integration can be applied to the mapping of the PMF in a much more general sense, as long as a certain parameter can be defined to link states of interest whose free-energies are to be calculated.

This chapter is organized as follows. In Sec. 6.1, we introduce principles underlying PMF exploration and the umbrella sampling, as well as the adaptive umbrella sampling methods. Then, we will explain a bit of the metadynamics method in

Sec. 6.2. The integrated tempering sampling method, as an example of enhanced sampling in which an *a priori* definition of transition coordinate is not required, is explained in Sec. 6.3. The thermodynamic integration method for the calculation of the free-energy of a certain phase is introduced in Sec. 6.4. We hope this introduction can help those graduate student started working on molecular simulations to set up some concepts before their enhanced sampling simulations were carried out.

6.1 Umbrella Sampling and Adaptive Umbrella Sampling Methods

A key concept for our understandings of the enhanced sampling method is the PMF as mentioned in the introduction, which was first given by Kirkwood in 1935 [289]. In this definition, a reaction coordinate ξ is used which is a function of the poly-atomic system's nuclear configuration in the Cartesian space. Here, we denote this spatial configuration of the nuclei as $\mathbf{x}$. It is a $3N$ dimensional vector composed by $\mathbf{x}^i$, with i going through 1 and N. $\mathbf{x}^i$ represents the Cartesian coordinate of the i^{th} nucleus and ξ can be written as $\xi(\mathbf{x})$. This nomenclature for the nuclear configuration will also be used for our discussions of the path-integral method in Chapter 7.

From the principles of statistical mechanics, one can first write down the free-energy profile of the poly-atomic system as a function of ξ, with the variable denoted by ξ_0, as:

$$\begin{aligned} F(\xi_0) &= -\frac{1}{\beta}\ln P(\xi_0) \\ &= -\frac{1}{\beta}\ln\frac{\int e^{-\beta V(\mathbf{x})}\delta(\xi(\mathbf{x})-\xi_0)d\mathbf{x}}{Q}. \end{aligned} \tag{6.1}$$

Here, β equals $1/(k_{\text{B}}T)$ and Q is the canonical partition function of the system:

$$Q = \int e^{-\beta V(\mathbf{x})}d\mathbf{x}. \tag{6.2}$$

ξ_0 is the variable used to construct the PMF. In the following discussion, we use a one-dimensional case as an example for simplicity. The extension of the equations to higher dimensional situations is straightforward. This PMF is a key function in descriptions of the configurational (or conformational) equilibrium properties as well as the transition rate of the dynamically activated processes in computer simulations for the behaviors of poly-atomic systems under finite temperatures.

From this definition of the PMF, one knows that it is closely related to the Born-Oppenheimer PES since the later, together with the thermal and quantum fluctuations of the nuclei, determine the probability distribution function $P(\xi_0)$ at a finite temperature. In other words, one can think of the PMF as a revised version of

the PES, with the thermal and quantum effects included in addressing the electronic and nuclear degrees of freedoms. In the introduction of this chapter, one can see that in cases when there exists multiple deep local minima on the PES, the probability distribution function $P(\xi_0)$ is far from being ergodic and one needs the enhanced sampling method to map out the PMF over the entire conformational space relevant to the problem of interest. Among the various efforts carried out in the last almost 4 decades, the umbrella sampling method first proposed by Torrie and Valleau is now believed to be one of the most influential [94, 95]. The mathematical basis for a treatment like this is that in order for an ergodic sampling of the conformational space relevant to the problem of interest, an additional biased potential $V_{\rm b}$ as a function ξ can be added to the real inter-atomic potential $V(\mathbf{x})$ in the molecular simulations. With this biased additional potential, a biased PMF can be constructed using:

$$\begin{aligned} F_{\rm b}(\xi_0) &= -\frac{1}{\beta}\ln P_{\rm b}(\xi_0) \\ &= -\frac{1}{\beta}\ln\frac{\int e^{-\beta(V(\mathbf{x})+V_{\rm b}(\xi(\mathbf{x})))\delta(\xi(\mathbf{x})-\xi_0)}d\mathbf{x}}{Q_{\rm b}}, \end{aligned} \tag{6.3}$$

where

$$Q_{\rm b} = \int e^{-\beta(V(\mathbf{x})+V_{\rm b}(\xi(\mathbf{x})))}d\mathbf{x}. \tag{6.4}$$

Due to the fact that the biased potential can be chosen in a way that $V(\mathbf{x})+V_{\rm b}(\xi(\mathbf{x}))$ is rather flat as a function of ξ (see Fig. 6.1), the probability distribution $P_{\rm b}(\xi_0)$ can be much better sampled over the whole conformational space relevant to the problem of interest compared with $P(\xi_0)$ in the MD simulations so that the biased PMF can be calculated efficiently using MD statistics.

Then, one relates the biased PMF $F_{\rm b}(\xi_0)$ with the unbiased one $F(\xi_0)$ using the following equation:

$$\begin{aligned} F_{\rm b}(\xi_0) &= -\frac{1}{\beta}\ln\frac{\int e^{-\beta(V(\mathbf{x})+V_{\rm b}(\xi(\mathbf{x})))\delta(\xi(\mathbf{x})-\xi_0)}d\mathbf{x}}{Q_{\rm b}} \\ &= -\frac{1}{\beta}\ln e^{-\beta V_{\rm b}(\xi_0)}\frac{\int e^{-\beta V(\mathbf{x})}\delta(\xi(\mathbf{x})-\xi_0)d\mathbf{x}}{Q_{\rm b}} \\ &= V_{\rm b}(\xi_0) - \frac{1}{\beta}\ln\left[\frac{\int e^{-\beta V(\mathbf{x})}\delta(\xi(\mathbf{x})-\xi_0)d\mathbf{x}}{Q}\frac{Q}{Q_{\rm b}}\right] \\ &= V_{\rm b}(\xi_0) - \frac{1}{\beta}\ln\frac{\int e^{-\beta V(\mathbf{x})}\delta(\xi(\mathbf{x})-\xi_0)d\mathbf{x}}{Q} - \frac{1}{\beta}\ln\frac{Q}{Q_{\rm b}} \\ &= V_{\rm b}(\xi_0) + F(\xi_0) - \frac{1}{\beta}\ln\frac{Q}{Q_{\rm b}}. \end{aligned} \tag{6.5}$$

Therefore, from the biased PMF $F_{\rm b}(\xi_0)$, which can be sampled well in practical MD simulations over the whole conformational space, one can reconstruct the unbiased

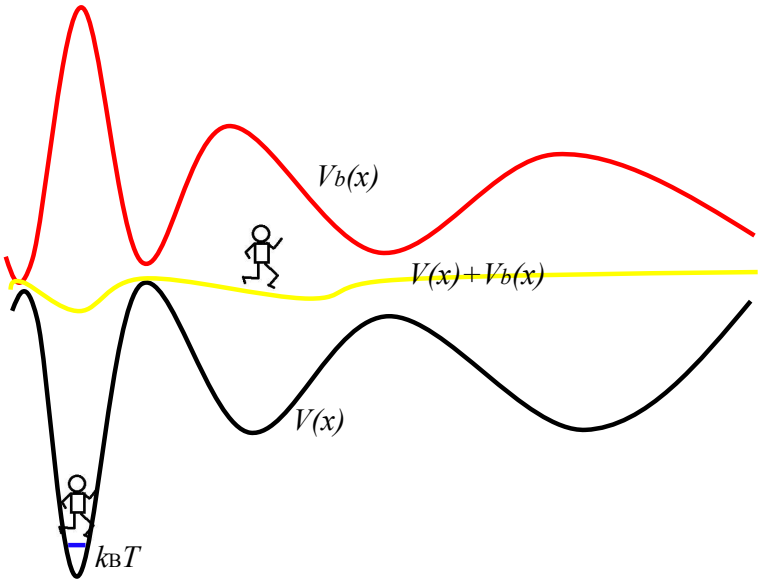

Figure 6.1: Taking the simplest case, *i.e.* the system is one dimensional and the ξ is the same as the x, as an example, the original PES $V(x)$ has a very deep valley so that the MD simulation can't go through the whole space in practical MD simulations. However, if an additional biased potential $V_b(x)$ which roughly equals $-V(x)$ is added to the original potential, the new potential $V_b(x) + V(x)$ will be very flat so that in a MD simulation using this potential the particle can through the whole x axis freely and $F_b(x)$ can be sampled very well. Based on this $F_b(x)$, the original free-energy profile can be reconstructed using Eq. 6.7. This principle also applies to system with higher dimensions for the nuclear degree of freedom and more complex form of the reaction coordinate ξ.

PMF through:

$$F(\xi_0) = F_{\mathrm{b}}(\xi_0) - V_{\mathrm{b}}(\xi_0) + \frac{1}{\beta} \ln \frac{Q_{\mathrm{b}}}{Q}. \tag{6.6}$$

We note that this $\frac{1}{\beta} \ln \frac{Q_{\mathrm{b}}}{Q}$ is a constant, which we denote as F. It is independent of ξ_0 but determined by the choice of $V_{\mathrm{b}}(\xi)$, the conformational space of the poly-atomic system relevant to the problem of interest, the original inter-atomic potential, and the temperature. Rewriting of Eq. 6.6 also gives us:

$$F(\xi_0) = F_{\mathrm{b}}(\xi_0) - V_{\mathrm{b}}(\xi_0) + F. \tag{6.7}$$

As simple as it looks, the addition of a biased potential easily solves the problem for the ergodic exploration of the conformational space for the mapping of the PMF in principle in the MD simulations. However, we note that in practical applications,

the high-dimensional PES function $V(\mathbf{x})$ is always unknown. Therefore, it is impossible to define an additional potential in the negative form of it in an *a priori* manner so that the system can go through the entire conformational space relevant to the problem of interest efficiently using this biased potential. When this is the case and the chosen additional potential doesn't compensate the original one, the system will still be trapped in one local minimum in the MD simulations under the biased potential (see e.g. Fig. 6.2).

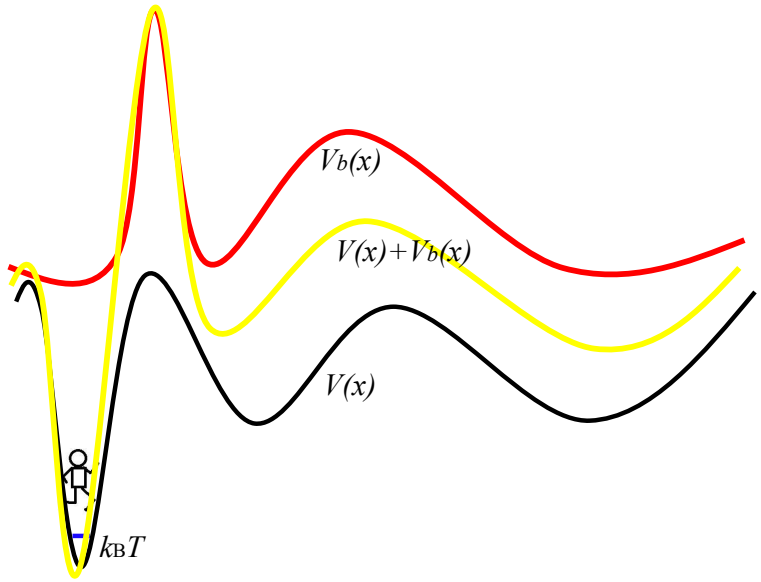

Figure 6.2: The situation is similar to Fig. 6.1. However, one doesn't know the form of the original potential and therefore the additional one doesn't compensate it well. In this case, the sampling of the system with the biased potential won't be ergodic on the conformational space either.

One way to circumvent this problem and ensure that the whole conformational space relevant to the problem of interest is sufficiently (or even uniformly) sampled is to separate this conformational space into some boxes using the chosen reaction coordinates. When there is only one reaction coordinate, this simplified into taking some values of ξ in the region relevant to the problem of interest, say ξ^i. Then, a series of MD simulations can be carried out using these biased potentials which constrain the system in the neighborhood of these ξ^is so that the conformational spaces of the system with reaction coordinates in the neighborhood of all these ξ^is are all well-sampled. Taking the one-dimensional PMF associated with two stable states (reactant and product) separated by a high energy barrier as an example (Fig. 6.3), in the language of Torrie and Valleau [94, 95], a series of bias potential can be used along the reaction path between the reactant and the product. At each point along

this path, a bias potential is used to confine the system to the neighborhood of it and the corresponding simulation is often called a "biased window simulation". From this simulation, one can reconstruct the PMF in this neighborhood from the MD simulation using the biased potential. Then, by link the PMF in each region, one obtains the PMF along the reaction coordinate all over the conformational space interested. We note that there can be many choices for this additional constraint potential. One of the most often used is the harmonic function with the form $V_{\mathrm{b}}^{i}(\xi_0) = \frac{1}{2}K(\xi_0 - \xi^i)^2$, as shown by the red curves in Fig. 6.3. Due to the fact that this additional bias potential looks like an umbrella (Fig. 6.3), this method is called the umbrella sampling in literature. With this treatment, a uniform series of sample points in the region relevant to the problem of interest will ensure that the conformational space is sufficiently sampled and consequently the PMF well-reconstructed.

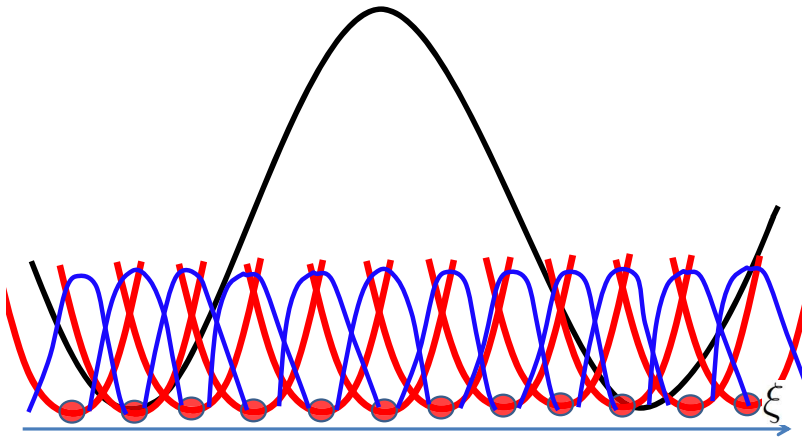

Figure 6.3: Illustration on how the umbrella sampling is used in simulations of the transition between a reactant state and a product one separated by high energy barrier. Along the reaction coordinate, a series of points were taken. At each point ξ_i, a bias potential with the form $V_{\mathrm{b}}(\xi) = \frac{1}{2}K(\xi - \xi_i)^2$ is used to constrain the system to its neighborhood. From this biased simulation, the PMF at this neighborhood can be obtained from the corresponding probability distribution (indicated by the blue curve). These series of additional biasing potential ensures that the whole conformation space relevant to the problem of interest is sufficiently sampled.

A main technical problem related to the reconstruction of the PMF from the umbrella sampling as mentioned above originates from the fact that in Eq. 6.7 there is a constant which depends on the choice of the additional potential and the region it explores. This indicates that this constant is different in each of the biased MD simulations. Consequently, one needs to align the PMF reconstructed

in each region of the simulation window so that the relative value of the PMF obtained from different MD simulations make sense. Traditionally, this is done by adjusting $F(\xi_0)$ of the adjacent boxes (windows) in which they overlap so that they match [94, 95, 96], using e.g. least-square method [290]. In so doing, the PMF over the whole region interested can be constructed. However, we note that there are serious limitations for this scheme. First, in matching the overlap region between the PMF of the neighboring windows, a significant overlap is required to ensure statistical accuracy. This indicates that a lot of sampling in the MD simulations are superfluous and consequently wasted. And more importantly, when more than one reaction coordinates are used for the construction of the PMF, the value of the constant F in one simulation window allowing the best fit with its adjacent region in one direction may not ensure the best for others [291]. Therefore, this scheme is of limited use in practical simulations of complex systems when analysis of high-dimensional PMF is required.

Among the various attempts to solve these problems [290, 292, 293, 294], the weighted histogram analysis method (WHAM) proposed by Kumar *et al.* is now the most popular, mainly due to its numerical stability and convenience in addressing PMF with multiple variables [295]. The central equation for the WHAM method resides in the optimization of the unbiased distribution function as a weighted sum over its expression in different windows, as:

$$P(\xi_0) = \sum_{i=1}^{N_\mathrm{w}} \left[P^i(\xi_0) \frac{n_i e^{-\beta(V_\mathrm{b}^i(\xi_0)-F_i)}}{\sum_{j=1}^{N_\mathrm{w}} n_j e^{-\beta(V_\mathrm{b}^j(\xi_0)-F_j)}} \right], \tag{6.8}$$

where N_w is the number of windows and $P^i(\xi_0)$ represents the unbiased probability distribution reconstructed from the biased MD simulation in the i^{th} window using $V_\mathrm{b}^i(\xi_0)$. Same as above discussions, ξ_0 denotes the variable and $V_\mathrm{b}^i(\xi_0) = \frac{1}{2}K(\xi_0 - \xi^i)^2$. $P(\xi_0)$ is the optimized overall distribution function obtained from the N_w biased simulations. This definition of $P(\xi_0)$ (instead of a direct sum over $P^i(\xi_0)$) is very reasonable since not only the relative weights between the number of independent data points within each window (*i.e.* n_i) is taken into account (more data better statistics and consequently larger weights in the summation), but also the small weights of $P^i(\xi_0)$ in the region with large $V_\mathrm{b}^i(\xi_0) - F_i$ means that the error originating from worse statistics of $P^i(\xi_0)$ in this region gets numerically well-under-control. This expression, together with the right values of the F_is (i goes from 1 to N_w), gives the unbiased distribution function of $P(\xi_0)$ throughout the regions on the ξ axes relevant to the conformational space interested. What one needs to do next is to optimize the values of F_is in Eq. 6.8.

To understand how this is done in practice, we go back to Eq. 6.7 for the biased MD simulation in each window. This equation changes to

$$F^i(\xi_0) = F_\mathrm{b}^i(\xi_0) - V_\mathrm{b}^i(\xi_0) + F^i, \tag{6.9}$$

where $F^i(\xi_0) = -\frac{1}{\beta}\ln P^i(\xi_0)$ and $F^i_{\rm b}(\xi_0) = -\frac{1}{\beta}\ln P^i_{\rm b}(\xi_0)$. $P^i_{\rm b}(\xi_0)$ represents the biased probability distribution sampled with the biased potential around ξ^i, which is directly obtained from the $i^{\rm th}$ MD simulations. Statistically, it samples the region around ξ^i rather well. By imputing the expressions of $F^i(\xi_0)$ and $F^i_{\rm b}(\xi_0)$ into Eq. 6.9, one gets:

$$P^i(\xi_0) = P^i_{\rm b}(\xi_0)e^{V^i_{\rm b}(\xi_0)-F^i}. \tag{6.10}$$

Therefore, Eq. 6.8 evolves into:

$$P(\xi_0) = \sum_{i=1}^{N_{\rm w}} \frac{n_i P^i_{\rm b}(\xi_0)}{\left[\sum_{j=1}^{N_{\rm w}} n_j e^{-\beta(V^j_{\rm b}(\xi_0)-F_j)}\right]}, \tag{6.11}$$

The free-energies F_is in Eq. 6.11, on the other hand, satisfy the following equation:

$$\begin{aligned} F_i &= -\frac{1}{\beta}\ln\frac{Q^i_{\rm b}}{Q} \\ &= -\frac{1}{\beta}\ln\frac{\int e^{-\beta(V(\mathbf{x})+V^i_{\rm b}(\xi(\mathbf{x})))}d\mathbf{x}}{Q} \\ &= -\frac{1}{\beta}\ln\int e^{-\beta V^i_{\rm b}(\xi_0)}P(\xi_0)d\xi_0. \end{aligned} \tag{6.12}$$

Therefore, Eq. 6.11 and Eq. 6.12 compose a set of equations which define the relationship between the F_is and $P(\xi_0)$. By solving these two equations self-consistently, one can obtain a much better and more efficient estimate of $P(\xi_0)$ compared with the traditionally PMF matching method from the statistical point of view. Once again, we note that the essence of this method, in the language of Roux [96], is "constructing an optimal estimate of the unbiased distribution function as a weighted sum over the data extracted from all the simulations and determining the functional form of the weight factors that minimizes the statistical error".

So far about the umbrella sampling method. From this introduction, we know that a key point on reconstructing the PMF using the biased potential is that a sufficient sampling, in the best case uniform sampling, of the conformational space relevant to the problem of interest is guaranteed. To this end, an *a priori* set of umbrella potentials are needed in order for this uniform sampling to be carried out in a practical manner. For simulations of relatively simple systems, in which the variable related to the umbrella potential is easy to define, this method works well. However, for complex systems where this *a priori* definition of the umbrella potential is unlikely, which unfortunately is usually true in reactions with more than 1 degree of freedom, this method often fails.

An alternative method within a similar scheme, which is more often used in present explorations of the PMF in complex systems, is the so-called adaptive umbrella sampling method [296, 297, 298]. A key difference between the adaptive

umbrella sampling method and the umbrella sampling method is that in the former case the umbrella potentials are chosen and updated in the simulations, while in the later one the umbrella potentials don't change. Plus, in the umbrella sampling method, the conformational space is separated into a series of regions and the MD simulation with bias potential centered at each region have different F_i. A key point to combine the PMFs constructed from the biased MD simulations in umbrella sampling is to align these different F_is. While in the adaptive umbrella sampling method, the umbrella potential doesn't focus a specific region but rather tries to compensate the original PES. Consequently, the problem related to the treatment of the constant in Eq. 6.7 transforms into shifting this value during the iterations so that in the end it equals the free-energy density of the system over the whole conformation space relevant to the study.

The central idea behind the adaptive umbrella sampling method is that if an umbrella potential with the form $V_{\mathrm{b}}(\xi_0)$ results in a uniform biased probability distribution $P_{\mathrm{b}}(\xi_0)$, the corresponding umbrella potential satisfies the following equation:

$$V_{\mathrm{b}}(\xi_0) = -V(\xi_0) = \frac{1}{\beta} \ln P(\xi_0), \tag{6.13}$$

where $P(\xi_0)$ stands for the unbiased probability distribution we want to simulate. Based on this equation, the biasing potential can be adapted to the PMF which is determined using the information from the previous simulations in an iterative manner [299]. The analysis of the PMF is often carried out using WHAM [295]. To be more specific, an initial guess of the umbrella potential, which is often taken as $V_{\mathrm{b}}^1(\xi_0) = 0$ can be used for the MD simulation and a biased probability distribution $P_{\mathrm{b}}^1(\xi_0)$ is obtained. From this biased probability distribution, one can construct the unbiased one ($P^1(\xi_0)$). Due to the ergodic problem related to the original PES, this $P^1(\xi_0)$ will be very different from the final $P(\xi_0)$. However, one can input this unbiased probability distribution into Eq. 6.13 and get a new umbrella potential $V_{\mathrm{b}}^2(\xi_0)$. Adding this biasing potential to the original potential and one can perform the second biased MD simulation and generate a new $P_{\mathrm{b}}^2(\xi_0)$. From this biased probability distribution, a normalized unbiased one $P^2(\xi_0)$ can be achieved. This unbiased potential will be summed up with the unbiased one in the first round subjecting to some normalized weighting factors to generate the new input for Eq. 6.13. From Eq. 6.13, again, one obtains a new umbrella potential. Continue this iteration and take care of the fact that the input for Eq. 6.13 is always generated using weighted sum over unbiased probability distributions obtained from earlier iterations, until the conformational space relevant to the problem of interest has been sampled adequately, one can get a well-converged unbiased PMF. This unbiased PMF can then be used for later statistical or dynamical studies. We note that this is just a general description of how the adaptive umbrella sampling works. There are many numerical details concerning real implementation. For these details, please refer to

Ref. [299, 300].

6.2 Metadynamics

In the above discussions on the umbrella sampling and adaptive umbrella sampling methods, Eq. 6.7 is the basis for the analysis to be carried out and rigorous justification for the construction of the unbiased PMF exists behind the biased MD simulations. Parallel to this scheme, however, there is another algorithm which (as pointed by A. Laio, a main founder of this method) didn't follow from any ordinary thermodynamic identity but was rather postulated on a heuristic basis and later verified empirically to be very successful in the enhanced sampling simulations of many complex systems [301, 302, 303, 304, 305, 306, 307]. This method is so-called metadynamics [38, 39].

The principles underlying this metadynamics method can be understood pictorially using Fig. 6.4. The first step is to choose a sensible collective variable (labelled as CV, corresponding to the reaction coordinate used in the earlier discussion) which in principle, should be able to distinguish the initial, intermediate, and final states and describe the slow processes relevant to the problem of interest. This is similar to the umbrella sampling and adaptive umbrella sampling methods as introduced before. The difference appears afterwards. Imagine that only one CV is chosen and the Born-Oppenherimer PES looks like the black curve in Fig. 6.4, starting from one deep valley, the system will take a time which is unacceptably long for atomic simulations to escape from it using the standard MD method. In the language of metadynamics, what one can do in order to impose an efficient enhanced sampling on the PES is to add in some additional potentials so that the deep valley can be filled up quickly (Fig. 6.4 (a)). This potential can be written in terms of Gaussian functions, as:

$$V_{\mathrm{G}}(\xi(\mathbf{x}),t) = w \sum_{t'=\tau_{\mathrm{G}},2\tau_{\mathrm{G}},\cdots \text{ and } t'<t} e^{-\frac{(\xi(\mathbf{x})-\xi(t'))^2}{2(\delta s)^2}}, \tag{6.14}$$

where $\xi(\mathbf{x})$ stands for the CV coordinate associated with the spatial configuration of the nuclei $\mathbf{x}$, and $\xi(t')$ stands for its instantaneous value at t'. It is obvious that the Gaussian height w, Gaussian width δs, and the time interval τ_{G} at which the Gaussians are added control the form of this additional potential and consequently the accuracy and efficiency of the enhanced sampling. Imagine that the Gaussian potentials are like small stones (size of the stone controlled by w and δs) which fill up the valley gradually, the difference between the red curve and the black curve then naturally represents the sum over the Gaussian functions as shown in Eq. 6.14. And the size of the stones determines the efficiency of accuracy for the construction of this difference between the red and black curves. After one valley

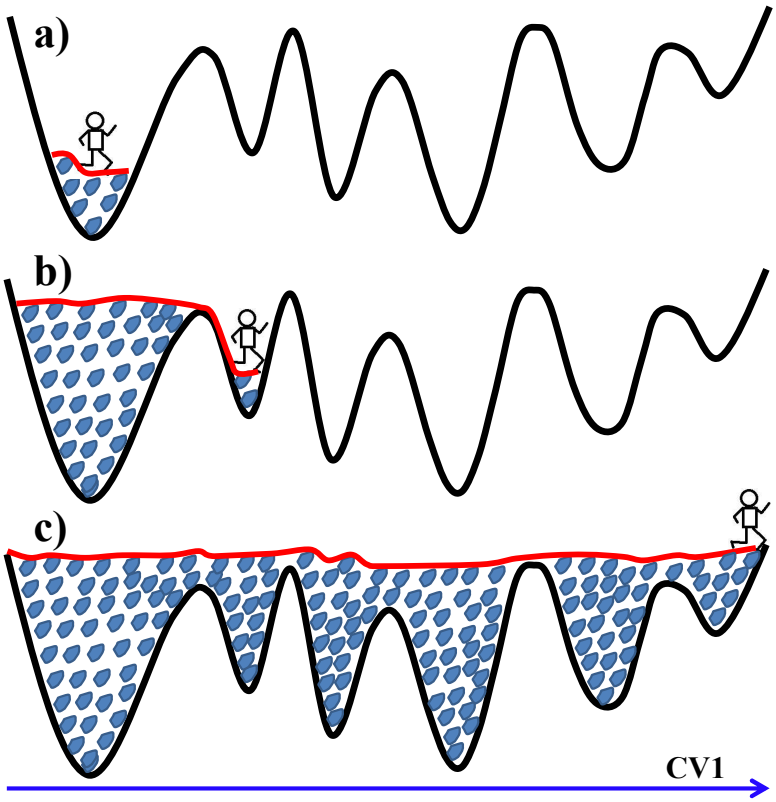

Figure 6.4: Illustration on the principles underlying the metadynamics method, taking the one dimensional case as an example. Imagine that the PES has multiple deep valleys. In metadynamics, some artificial potentials will be added along the chosen collective variable coordinates as the system evolves. At a certain valley, this is similar to the case that a man fails into a deep well. To get out of it, simply by jumping is unlikely, but imaging that he has an infinite account of stones in his "magic" pocket, he can throw a stone every few steps he walks. With time going on, these stones will fill up the well and he can get out of it easily. By remembering the geometric shape of the space filled up by the stone, intuitively the PMF can be reconstructed. It is easy to understand that the size of the stone determines the accuracy and efficiency for the PMF reconstructed. As mentioned in the main text, this rationalization is postulated on a heuristic basis. However, we note that it has been verified empirically to be very successful in the enhanced sampling simulations of many complex systems [301, 302, 303, 304, 305, 306, 307].

was filled up, the walker which describes the evolution of the system in the enhanced sampling process starts to explore the neighboring one (Fig. 6.4 (b)), until all the valleys were filled. After that, the system is allowed to travel between the valleys

in a free manner (Fig. 6.4 (c)). When the exploration of the walker is controlled using an ensemble based method, such as the molecular dynamics or the Monte-Carlo algorithm, the random walking above all the barriers will naturally include thermal fluctuations and entropy. Consequently, if a canonical ensemble is used, the difference between the red curve (which is not flat) and the blue curve intuitively reflects the profile for the PMF. As a result, the following equality exists:

$$F(\xi) = -\lim_{t\to\infty} V_{\mathrm{G}}(\xi, t). \tag{6.15}$$

This equation serves as the basic assumption of metadynamics. In practice, many details exist concerning the implementation of the algorithm described above. The readers please refer to Ref. [39] for a detail explanation. We note that from the first sight, this metadynamics looks similar to the adaptive umbrella sampling, due to the fact that the sum of the Gaussian functions gradually gives us the PMF using Eq. 6.15. In the adaptive umbrella sampling method, a gradual history dependent improvement on the assessment of the PMF also exists by going through the iterations. However, we note that the philosophy is very different. In the adaptive sampling method, the update of the PMF using Eq. 6.13 has a rigorous justification. While in the metadynamics, the construction of the PMF using Eq. 6.15 is postulated on a heuristic basis. This postulation was later verified empirically in several systems with increasing complexity, as can be seen for example, in Refs. [38, 39, 301, 302, 303, 304, 305, 306, 307].

6.3 Integrated Tempering Sampling

In all methods introduced above, one or more reaction coordinates are required in order to describe the atomistic level evolution of the system in its conformational space. By increasing the complexity of the poly-atomic system, however, it can easily happen that the definition of such reaction coordinates becomes difficult or even impossible. In these cases, another kind of methods, which effectively avoid an *a priori* selection of the reaction coordinates, serve as an alternative. In these methods, a commonly used technical trick is to alter the potential energy landscape using the temperature or energy itself, so that the the exploration of the conformational space can be accelerated and the preselection of the transition coordinates is avoided. One of the earliest example is the Tsallis statistical method proposed in the late 1980s [308]. In this method, a high temperature sampling, which can be viewed as an exploration of the "potential energy surface scaled by temperature", does enforce an enhanced sampling of the rare events. However, due to the relatively primitive algorithm, the high temperature regions, which do not play an important role at the targeting temperature of the canonical ensemble under investigation, can be easily over-sampled [309]. To improve on this, a series of methods were developed in the

last two decades, with the Wang-Landau [310, 311], replica exchange [34, 35, 36, 37], integrated tempering sampling (ITS) [44, 45, 46], and selective integrated tempering sampling (SITS) [312] methods being the most prominent successful examples. Among them, the Wang-Landau method possesses a uniform distribution on the energy scale, which is very suitable for the Monte-Carlo simulations. The replica exchange, ITS, and SITS are presently very often used methods in the MD simulations. A thorough description for all of them is beyond the scope of this chapter. Here, we will take the ITS method as an example to show how such enhanced samplings are realized when the exploration of the PMF focusses on the energy space in the MD simulations.

The ITS method is intrinsically temperature-based, in which a generalized non-Boltzmann ensemble is used. This generalized non-Boltzmann ensemble allows an enhanced sampling in a desired broad energy and temperature range. The key quantity is a distribution function of the inter-atomic potential. It is defined as an integral or summation of the Boltzmann terms over temperature, through:

$$p(U) = \sum_{k=1}^{M} n_k e^{-\beta_k U}, \tag{6.16}$$

where U stands for the physical inter-atomic interaction potential and $\beta_k = 1/(k_{\mathrm{B}}T_k)$. M is the number of temperatures used for the summation over the Boltzmann distribution. T_k means the temperature used in each of them, which increases with k from T_1 to T_M. The highest temperature used (T_M) is determined by the height of the barrier and the associated time-scale one wants to simulate. n_k is a weight. It is determined through the requirement that each term in the summation in Eq. 6.16 contributes a desired fraction of the system's Boltzmann distribution (at a given temperature T_k) to the total non-Boltzmann one.

In order to allow a MD based method to sample the distribution function in Eq. 6.16, one must impose an equality between a Boltzmann-like distribution function and the non-Boltzmann one in Eq. 6.16, at a targeting temperature T (with the corresponding β equals $1/(k_{\mathrm{B}}T)$). To this end, the inter-atomic potential must be revised. Let's assume that this revised form of the inter-atomic potential is $U^{'}$, then, the requirement that the distribution function $p(U)$ in Eq. 6.16 can be reproduced by a finite temperature MD simulation imposes:

$$e^{-\beta U^{'}} = p(U) = \sum_{k=1}^{M} n_k e^{-\beta_k U}. \tag{6.17}$$

From this equality, one easily obtains:

$$U^{'} = -\frac{1}{\beta} \ln \left[\sum_{k=1}^{M} n_k e^{-\beta_k U} \right]. \tag{6.18}$$

And consequently, the biased force $\mathbf{F}_\mathrm{b}$ on the i^{th} atom can be calculated from:

$$\mathbf{F}_\mathrm{b}^i = \frac{\sum_{k=1}^{M} n_k \beta_k e^{-\beta_k U}}{\beta \sum_{k=1}^{M} n_k e^{-\beta_k U}} \mathbf{F}^i, \tag{6.19}$$

where $\mathbf{F}_i$ stands for the Hellmann-Feynman force on the i^{th} nuclei when the inter-atomic potential is the physical one (namely U).

From Eqs. 6.17 to 6.19, it is clear that a MD simulation using a Boltzmann-ensemble (but with an "artificial" inter-atomic potential) can be employed to reproduce the distribution function associated with the non-Boltzmann ensemble in Eq. 6.16. Due to the fact that a wide temperature range is included in the summation over the Boltzmann distribution function in Eq. 6.16 for the non-Boltzmann ensemble, it is expected that the probability of the rare event, which hardly happens in a normal MD simulation at the targeting physical temperature, can be increased. However, one notes that there are still some weighting factors to be determined in Eq. 6.19. These factors are determined through the requirement that each term in the summation of Eq. 6.16 contribute to the total distribution with a desired fraction. In other words, if one defines

$$P_k = n_k \int e^{-\beta_k U(\mathbf{x})} d\mathbf{x}, \tag{6.20}$$

where $\mathbf{x}$ stands for a $3N$-dimensional vector in the conformation space (N means the number of nuclei in the poly-atomic system), each term in the summation of Eq. 6.16 will contribute to the total distribution with a fraction

$$p_k = \frac{P_k}{\sum_{k=1}^{M} P_k}. \tag{6.21}$$

These p_ks should be aimed at some predetermined quantities with which we want our finite temperature (T_k) Boltzmann distribution contributes to the non-Boltzmann one. Let's label such a fraction as p_k^0. In practice, the fraction that all these p_k^0s equal $1/M$ is often used.

With these predetermined p_k^0s, an initial guess for the numbers n_k will be employed in the first a certain number of, say N_τ, MD steps using the forces generated by Eq. 6.19. The targeting temperature is T. At the end of these N_τ steps, the values of p_k will be calculated using Eqs. 6.20 and 6.21. It is often true that these p_ks are different from their targeting values p_k^0s. To ensure that they fluctuate around and approach their targeting values with the simulation going on, in the next N_τ steps, the value of n_k will be changed into its original value multiplied by p_k^0/p_k. At the end of these N_τ steps, the values of p_k will be calculated again and the values of n_k are updated by the same relation. With the simulation going on, a sufficient

sampling of the non-Boltzmann in Eq. 6.16 will be guaranteed. We note that this algorithm reflects only the principles underlying the ITS method. In practical applications, there are more reliable algorithms used. For these technical details, please refer to Gao, Yang, Fan, and Shao's work in Refs. [44, 46].

6.4 Thermodynamic Integration

In the earlier sections, we have introduced some extensions of the MD method as presented in Chapter 5, by mainly focussing on the mapping of the PMF. Another problem which can be studied using the MD simulation technique concerns the phase behavior of a given substance, in particular, transitions between two competing phases obtained from either random structure searching or enhanced sampling molecular dynamics simulations. Melting from a solid to a liquid phase is one example. And evaluation of the relative stability between two competing solid phases is another one. In these examples, the transition between the two competing phases is first-order and their transition curve can be calculated from the principle that at coexistence the Gibbs free-energies of the two phases are equal. Here, we will introduce a method to calculate the free-energy of a given phase at a finite temperature and pressure so that such phase transitions can be studies in terms of molecular simulations. We note that continuous transitions, which will not be discussed here, are by no means simpler. We refer the readers to Ref. [313] if you are interested.

The method we want to introduce here is called the thermodynamic integration method [48, 49, 50, 51, 52, 53, 54, 55, 56, 57, 58, 280]. To be pediatric, we start by interpreting the principles underlying it and then explain some technical details. The key point of this method is that it is a general method to determine the free energy difference $F_1 - F_0$ between two systems whose total-energy functions are known, which we denote as U_1 and U_0. By total energy function, we mean that for a specific spatial configuration of the nuclei $(\mathbf{R}_1, \cdots, \mathbf{R}_N)$, the total energy of the first system is $U_1(\mathbf{R}_1, \cdots, \mathbf{R}_N)$ while the total energy for the second system is $U_0(\mathbf{R}_1, \cdots, \mathbf{R}_N)$. From the definition of the Helmholtz free-energy, it is determined by these total energy functions through

$$\begin{aligned} F_1 &= -k_{\mathrm{B}}T \ln \left\{ \frac{1}{N!\Lambda^{3N}} \int d\mathbf{R}_1 \cdots d\mathbf{R}_N e^{-\beta U_1(\mathbf{R}_1, \cdots, \mathbf{R}_N)} \right\}, \\ F_0 &= -k_{\mathrm{B}}T \ln \left\{ \frac{1}{N!\Lambda^{3N}} \int d\mathbf{R}_1 \cdots d\mathbf{R}_N e^{-\beta U_0(\mathbf{R}_1, \cdots, \mathbf{R}_N)} \right\}, \end{aligned} \tag{6.22}$$

where $\Lambda = h/(2\pi M k_{\mathrm{B}}T)^{1/2}$ is the thermal wavelength and M is the nuclear mass. For a simple nomenclature, we have assumed that all the nuclei have the same mass, but we note that the extension of Eq. 6.22 to systems with nuclei of different kinds is straightforward for the illustration of the principles to be discussed below.

By thermodynamic integration, we mean that if one imposes a series of fictitious systems in between the ones with free-energy F_1 and F_0, with the total energy function

$$U_\lambda(\mathbf{R}_1, \cdots, \mathbf{R}_N) = U_0(\mathbf{R}_1, \cdots, \mathbf{R}_N) + \lambda(U_1(\mathbf{R}_1, \cdots, \mathbf{R}_N) - U_0(\mathbf{R}_1, \cdots, \mathbf{R}_N)), \tag{6.23}$$

F_1 can be calculated with a thermodynamic integration treatment if F_0 is known. The mathematical foundation underlying this thermodynamic integration treatment is that for one specific value of λ, there is a total energy function $U_\lambda(\mathbf{R}_1, \cdots, \mathbf{R}_N)$ and a free-energy F_λ. It is clear from the definition of $U_\lambda(\mathbf{R}_1, \cdots, \mathbf{R}_N)$ in Eq. 6.23 that F_λ equals F_0 if λ equals zero, and it equals F_1 if λ equals one. Therefore, one can plot the evolution of F_λ as a function of λ in between zero and one, with the value of F_λ starting from F_0 and ending at F_1. Using this evolution, it is clear that

$$F_1 - F_0 = \int_0^1 \frac{dF_\lambda}{d\lambda} d\lambda. \tag{6.24}$$

This is pictorially shown in Fig. 6.5.

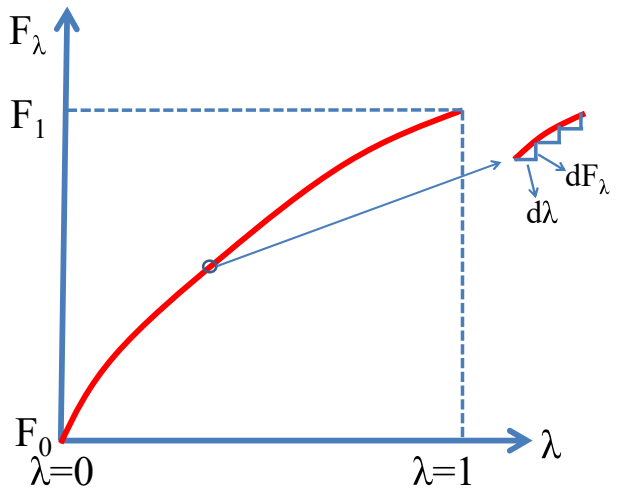

Figure 6.5: Illustration on the evolution of F_λ in the thermodynamic integration method. The x axis corresponds to the variable λ, which goes from 0 to 1. The y axis corresponds to the function F_λ, which goes from F_0 to F_1. F_0 is known while F_1 is unknown, which equals $F_0 + \int_0^1 \frac{dF_\lambda}{d\lambda} d\lambda$.

Now we look at $dF_\lambda/d\lambda$, similar to Eq. 6.22, F_λ is defined as

$$F_\lambda = -k_B T \ln \left\{ \frac{1}{N!\Lambda^{3N}} \int d\mathbf{R}_1 \cdots d\mathbf{R}_N e^{-\beta U_\lambda(\mathbf{R}_1, \cdots, \mathbf{R}_N)} \right\}. \tag{6.25}$$

Therefore, $dF_\lambda/d\lambda$ equals

$$\frac{dF_\lambda}{d\lambda} = -k_{\rm B}T \ln \left\{ \frac{1}{N!\Lambda^{3N}} \int d\mathbf{R}_1 \cdots d\mathbf{R}_N \frac{dU_\lambda(\mathbf{R}_1, \cdots, \mathbf{R}_N)}{d\lambda} e^{-\beta U_\lambda(\mathbf{R}_1, \cdots, \mathbf{R}_N)} \right\} \quad (6.26)$$

If one resort to the definition of U_λ in Eq. 6.23, it further equals

$$\frac{dF_\lambda}{d\lambda} = -k_{\rm B}T \ln \left\{ \frac{1}{N!\Lambda^{3N}} \int d\mathbf{R}_1 \cdots d\mathbf{R}_N (U_1(\mathbf{R}_1, \cdots, \mathbf{R}_N) - U_0(\mathbf{R}_1, \cdots, \mathbf{R}_N)) e^{-\beta U_\lambda(\mathbf{R}_1, \cdots, \mathbf{R}_N)} \right\}. \quad (6.27)$$

In other words, by putting Eq. 6.27 and Eq. 6.24 together, one arrives at

$$F_1 - F_0 = \int_0^1 d\lambda < U_1(\mathbf{R}_1, \cdots, \mathbf{R}_N) - U_0(\mathbf{R}_1, \cdots, \mathbf{R}_N) >_\lambda . \quad (6.28)$$

By $<>_\lambda$, we mean that the thermal average of the quantity to be evaluated is calculated using an ensemble average this quantity in a system with atomic interactions $U_\lambda(\mathbf{R}_1, \cdots, \mathbf{R}_N)$. Base on this deduction, it is clear that if the free-energy of a system with total energy function $U_0(\mathbf{R}_1, \cdots, \mathbf{R}_N)$ is known, one can calculate the free-energy of another system with total energy function $U_1(\mathbf{R}_1, \cdots, \mathbf{R}_N)$, by thermodynamically integrating the free-energy difference between F_1 and F_0.

Now we go to real poly-atomic systems. The definition of the thermodynamic integration as defined in Eq. 6.28 is robust, which means that as long as one has a good reference energy F_0, the free-energy of the real system F_1 can be calculated, through a continuous and isothermal switching of the total energy function from $U_0(\mathbf{R}_1, \cdots, \mathbf{R}_N)$ to $U_1(\mathbf{R}_1, \cdots, \mathbf{R}_N)$. However, we note that the efficiency of this thermodynamic integration sensitively depends on the similarity between the reference system and the system to be calculated. Mathematically, one can relate this similarity to the value of $U_1(\mathbf{R}_1, \cdots, \mathbf{R}_N) - U_0(\mathbf{R}_1, \cdots, \mathbf{R}_N)$ being evaluated in Eq. 6.27. The smaller this value, the fewer steps one needs to integrate for the value of λ between zero and one in Eq. 6.28.

Traditionally, this thermodynamic integration method has been extensively used in the molecular simulations with empirical inter-atomic potentials in the 1980s and 1990s [48, 49, 50, 51, 52, 53, 54]. In studies of liquids, this reference system is often taken as the idea gas with Lennard-Jones potential. While in studies of solids, this reference system is often chosen as the harmonic lattice. Starting from the 1990s, molecular simulations based on an *ab initio* treatment of the electronic structures have overtaken the traditional method in calculations of such free-energies, due to its power in describing inter-atomic interactions under complex chemical environments [55, 56, 57, 58, 280]. Since these *ab initio* calculations are much more expensive than the empirical potential calculations, it is highly recommended that one introduces an intermediate state between the idealized system with a rigorous

analytical expression for the free-energy and the real system [55, 280]. Due to the fact that a well-designed intermediate state held together by a well-defined empirical potential can be much similar to the real system compared with the idealized model, the thermodynamic integration between this intermediate state and the real one needs less value of λ in Eq. 6.28. As a compensate, more thermodynamic integration steps will be needed from the idealized model to the intermediate state. However, since the computational load for empirical potential based MD simulations is much smaller, this treatment can help us to save a lot of computation time, with errors well-in-control.

Till now, the principles underlying the thermodynamic integrations is clear. In the following, we use the free-energy of a crystal, with electronic structures determined by the density-functional theory calculations, as an example to show how this is done in practice [55, 280]. We note that the treatment of the nuclear motion in this thermodynamic integration is classical. Its extensions to the quantum nuclei will be discussed in Sec. 7.3 by resorting to the path-integral method as will be introduced in Chapter 7. In the *ab initio* MD based thermodynamic-integration calculations to be discussed here, the first key quantity is the electronic free-energy $U(\mathbf{R}_1, \cdots, \mathbf{R}_N; T_{\rm el})$. Compared with the total energy function $U(\mathbf{R}_1, \cdots, \mathbf{R}_N)$ we have used in the earlier discussions, one may notice two differences. The first one is that we prefer the word "free-energy" here while in the earlier discussions we use the word "total energy". The second difference is that there is one more parameter-dependence of this total energy, on $T_{\rm el}$, which denotes the temperature of the electrons. The physical origin of these two differences is the thermal electronic excitations in calculations of the electronic structures, which might be important in some situations [55, 280]. In many practical calculations of the density-functional theory, a smearing factor is used to generate partially occupied orbitals so that the electronic structures can be converged faster. We note that the smearing factor used there is not necessarily related to the real electron temperature. But here, by $T_{\rm el}$, we really mean the electron temperature which is determined by the environment. The corresponding electronic structure calculations should resort to the finite-temperature density-functional theory developed by N. D. Mermin in the 1960s [30, 31, 32]. Therefore, the total energy function $U(\mathbf{R}_1, \cdots, \mathbf{R}_N)$ becomes the electronic free-energy $U(\mathbf{R}_1, \cdots, \mathbf{R}_N; T_{\rm el})$, since the electronic entropy effects are naturally included in this finite-temperature density-functional theory. Accordingly, $T_{\rm el}$-dependency of this quantity enters. We note that this electronic free-energy equals

$$U(\mathbf{R}_1, \cdots, \mathbf{R}_N; T_{\rm el}) = E(\mathbf{R}_1, \cdots, \mathbf{R}_N; T_{\rm el}) - T_{\rm el} S, \tag{6.29}$$

where

$$E(\mathbf{R}_1,\cdots,\mathbf{R}_N;T_{\rm el}) = \sum_i f_i \int d\mathbf{r}\psi_i^*(\mathbf{r})\left(-\frac{1}{2}\nabla^2\right)\psi_i(\mathbf{r}) + \int n(\mathbf{r})V_{\rm ext}(\mathbf{r})d\mathbf{r} + \frac{1}{2}\int\int \frac{n(\mathbf{r})n(\mathbf{r}')}{|\mathbf{r}-\mathbf{r}'|}d\mathbf{r}d\mathbf{r}' + E^{\rm xc}\left[n(\mathbf{r})\right] + E_{\text{ion-ion}}(\mathbf{R}_1,\cdots,\mathbf{R}_N), \tag{6.30}$$

and

$$S = -2k_{\rm B}T\sum_i \left[f_i\ln f_i + (1-f_i)\ln(1-f_i)\right]. \tag{6.31}$$

In Eqs. 6.30 and 6.31, f_i is the Fermi-Dirac occupation number of the Kohn-Sham orbital ψ_i at $T_{\rm el}$ and $n(\mathbf{r}) = \sum_i f_i|\psi_i(\mathbf{r})|^2$. This Eq. 6.30 can be thought of as a finite-temperature version of the total-energy functional for the electronic system as introduced in Eq. 2.30, with nuclei interactions added. Such a treatment ensures that $U(\mathbf{R}_1,\cdots,\mathbf{R}_N;T_{\rm el})$ includes the electronic entropy effects and corresponds to the free-energy of the whole system with static nuclei at a certain spatial configuration $(\mathbf{R}_1,\cdots,\mathbf{R}_N)$. Therefore, for the nuclear system, it is just the total energy. Since this energy depends on $T_{\rm el}$, we use $U(\mathbf{R}_1,\cdots,\mathbf{R}_N;T_{\rm el})$ to label this total energy function of the nuclear configuration, with the free-energy of the electronic system completely included at the finite-temperature density-functional theory level.

With this total energy function in hand, we can calculate the Helmholtz free-energy. The first thing we do is to separate the total energy function into two parts, *i.e.* the static energy at the perfect-lattice positions $U(\mathbf{R}_1^0,\cdots,\mathbf{R}_N^0;T_{\rm el})$ and the remainder, through:

$$U(\mathbf{R}_1,\cdots,\mathbf{R}_N;T_{\rm el}) = U(\mathbf{R}_1^0,\cdots,\mathbf{R}_N^0;T_{\rm el}) + U^{\rm vib}(\mathbf{R}_1,\cdots,\mathbf{R}_N;T_{\rm el}). \tag{6.32}$$

$U(\mathbf{R}_1^0,\cdots,\mathbf{R}_N^0;T_{\rm el})$ is a constant which doesn't depend on $(\mathbf{R}_1,\cdots,\mathbf{R}_N)$. Therefore, the free-energy of the crystal, as determined by:

$$F = -k_{\rm B}T\ln\left\{\frac{1}{N!\Lambda^{3N}}\int d\mathbf{R}_1\cdots d\mathbf{R}_N e^{-\beta(U(\mathbf{R}_1^0,\cdots,\mathbf{R}_N^0;T_{\rm el})+U^{\rm vib}(\mathbf{R}_1,\cdots,\mathbf{R}_N;T_{\rm el}))}\right\}, \tag{6.33}$$

equals

$$F = U(\mathbf{R}_1^0,\cdots,\mathbf{R}_N^0;T_{\rm el}) - k_{\rm B}T\ln\left\{\frac{1}{N!\Lambda^{3N}}\int d\mathbf{R}_1\cdots d\mathbf{R}_N e^{-\beta U^{\rm vib}(\mathbf{R}_1,\cdots,\mathbf{R}_N;T_{\rm el})}\right\}. \tag{6.34}$$

From this equation, it is clear that the key issue resides in determining the second term in Eq. 6.34, which we label as $F^{\rm vib}$. This quantity, again, can be separated into two terms, *i.e.* $F^{\rm harm}$ which represents the free-energy of a harmonic lattice and

the deviation of F^{vib} from it. In terms of thermodynamic integration, the reference state is the harmonic lattice, whose free-energy can be calculated analytically using:

$$F^{\text{harm}} = \frac{3k_{\text{B}}T}{N_{\mathbf{k},s}} \sum_{\mathbf{k},s} \ln \left[e^{\frac{1}{2}\beta\hbar\omega_{\mathbf{k},s}} - e^{-\frac{1}{2}\beta\hbar\omega_{\mathbf{k},s}} \right], \tag{6.35}$$

where $\omega_{\mathbf{k},s}$ means the phonon frequency of branch s at reciprocal space point $\mathbf{k}$. The deviation of F^{vib} from F^{harm}, which we label as F^{anharm}, needs to be calculated using thermodynamic integration. From our discussions about, this term equals

$$F^{\text{anharm}} = \int_0^1 d\lambda < U^{\text{vib}}(\mathbf{R}_1, \cdots, \mathbf{R}_N) - U^{\text{harm}}(\mathbf{R}_1, \cdots, \mathbf{R}_N) >_\lambda . \tag{6.36}$$

Here, $U^{\text{harm}}(\mathbf{R}_1, \cdots, \mathbf{R}_N)$ means the harmonic potential associated with the Hessian matrix of the crystal. In some cases, to decrease computational load, an intermediate state can also be used, but the principles underlying these calculations for the free-energy of a crystal is already there. For more details, the readers please refer to Ref. [55].